

Supporting information

A Nanoporous Hygroscopic Pectin-Based Sorbent for Atmospheric Water Harvesting

Sonali Seth^a, Ankit Nagar^a, Tanmayaa Nayak^a, Vivek Yadav^a, Sujan Manna^a, and Thalappil Pradeep^{*a,b}

^aDST Unit of Nanoscience (DST UNS) and Thematic Unit of Excellence (TUE), Department of Chemistry, Indian Institute of Technology Madras, Chennai 600036, India.

^bInternational Centre for Clean Water, IIT Madras Research Park, Chennai 600113, India.

* Email: pradeep@iitm.ac.in

Supporting information content

Total number of pages: 19

Total number of figures: 12

Total number of tables: 1

Table of Contents

Items	Title	Page No.
	Experimental Section	S3-S4
Figure S1	FTIR spectra for the conversion of PC to PT.	S5
Figure S2	FTIR spectra for the conversion of AA to PA using MBA as the cross-linker, via free radical polymerisation.	S6
Figure S3	FTIR spectra for the functionalization of PC with AA using MBA as the cross-linker, via free radical polymerisation.	S7
Figure S4	Grafting of PT to AA using MBA as the cross-linker.	S8
Figure S5	FESEM images of PC, PA and PCPA.	S9
Figure S6	TGA thermograms of PC, PA, PCPA and PTPA under nitrogen atmosphere from room temperature to 800 °C.	S10
Figure S7	Sorption behaviour of PTPA at 293 K.	S11
Figure S8	The surface temperature distribution of PTPA under 1 Sun. The colour gradient is indicated on the right. Temperatures at various points are marked.	S13
Figure S9	FTIR of PTPA freshly prepared and after keeping in normal environmental conditions for 1 month.	S14
Figure S10	PTPA under 99% RH for 7 days.	S15
Figure S11	Time-dependent ATR-IR spectra of PTPA at regular time intervals on exposure to 99% RH.	S16
Figure S12	a) Deconvoluted Raman spectra of PTPA after 240 min of exposure to 99% RH. b) Schematic illustration for the water sorption by PTPA.	S17
Table S1	Comparison of the adsorbents costs and water production across different studies, based on lab-scale experiments.	S18
	References	S19

Experimental section

Materials

Pectin (PC), N, N'-methylenebisacrylamide (MBA), and potassium persulfate ($K_2S_2O_8$) were purchased from SRL Pvt. Ltd., India. Acrylic acid (AA, 99%) was obtained from Thermo Fisher Scientific India Pvt. Ltd., India. Potassium hydroxide (KOH) was purchased from Merck Life Science Pvt. Ltd., India, and sodium hydroxide (NaOH) from Thermo Fisher Scientific India Pvt. Ltd., India. Methanol was obtained from. Deionised (DI) water was used throughout the synthesis of hydrogels. All chemicals were of laboratory grade and used as received without further purification.

Methods

Synthesis of Pectin-Polyacrylic acid (PCPA)

PCPA sorbent was synthesised via free radical polymerisation by dissolving AA (5 g) in DI water (5 mL), followed by pH adjustment to 11 using NaOH. PC (7 wt% in DI water) was added to AA under constant stirring at room temperature in a two-neck round-bottom flask under N_2 atmosphere. MBA (200 mg) was further introduced as a cross-linker, and the mixture was heated to 70 °C. Free radical polymerisation was initiated by adding $K_2S_2O_8$ (500 mg), with the temperature gradually increased from 70 °C to 80 °C over 2 h. The obtained gel was purified by washing with a methanol-water mixture (80:20 v/v) and subsequently freeze-dried.

Synthesis of Pectate-Polyacrylic acid (PTPA)

Pectate (PT) was obtained by treating PC with 10% (w/v) KOH at 80 °C under constant stirring for 12 h. The resulting PT gel was centrifuged, thoroughly washed with DI water, and freeze-dried. The PTPA sorbent was then synthesised by functionalizing PT with AA under identical reaction conditions as PCPA, using MBA as the cross-linker. The obtained gel was purified by washing with a methanol-water mixture (80:20 v/v) and subsequently freeze-dried, which resulted in a porous granular morphology. These granules were directly used for the sorption studies due to their enhanced surface area and mass transfer properties.

Synthesis of Polyacrylic acid (PA)

For comparison, PA sorbent was synthesised under identical conditions as PCPA without PC.

Instrumentation

Scanning electron microscope (SEM) - Surface morphology was examined using an FEI Quanta 200 system. The samples were mounted on aluminium stubs and sputtered with gold prior to imaging.

Infrared (IR) - Surface chemical analysis was performed on a PerkinElmer FT-IR spectrometer with a resolution of 4 cm⁻¹.

Freeze Drying - Freeze drying of the samples were done using Eyela freeze dryer (Model No: FDU-1200).

X-ray Photoelectron Spectroscopy (XPS) - XPS measurement of the sample was conducted on ESCA Probe TPD system equipped with Mg K α X-ray source (h ν = 1253.6 eV).

Thermogravimetric Analysis (TGA) - Thermal analysis was performed using TA Instruments Q500 Thermogravimetric Analyzer. The measurements were carried out under nitrogen atmosphere from room temperature to 800 °C.

Water Sorption and Desorption Studies

Humidity uptake experiments were performed in the laboratory under ambient temperature of 25 ± 1 °C. Different RH conditions were maintained in a closed desiccator. Wet cotton was used to maintain 99% RH. Moisture uptake studies were done by recording the mass change at half-hour intervals for 12 h and subsequently at hourly intervals for the next 36 h. Moisture uptake was calculated using the equation (a)

$$\text{Moisture uptake} = (M_w - M_d) \div M_d \quad (\text{a})$$

Where M_w represents the mass of the sorbent after humidity uptake at different time intervals, and M_d represents the mass of the dry sorbent.

The CaCl₂ solution was used to maintain 35% (±1) RH in the desiccator. Similarly, 50% RH was maintained in the desiccator, and mass change was recorded at half-hour intervals for 6 h and subsequently at hourly intervals for the next 6 h.

Dynamic Vapor Sorption analyser – Sorption analysis was done using DVS analyzer (Hidden Isochema, UK).

Supporting Information 1

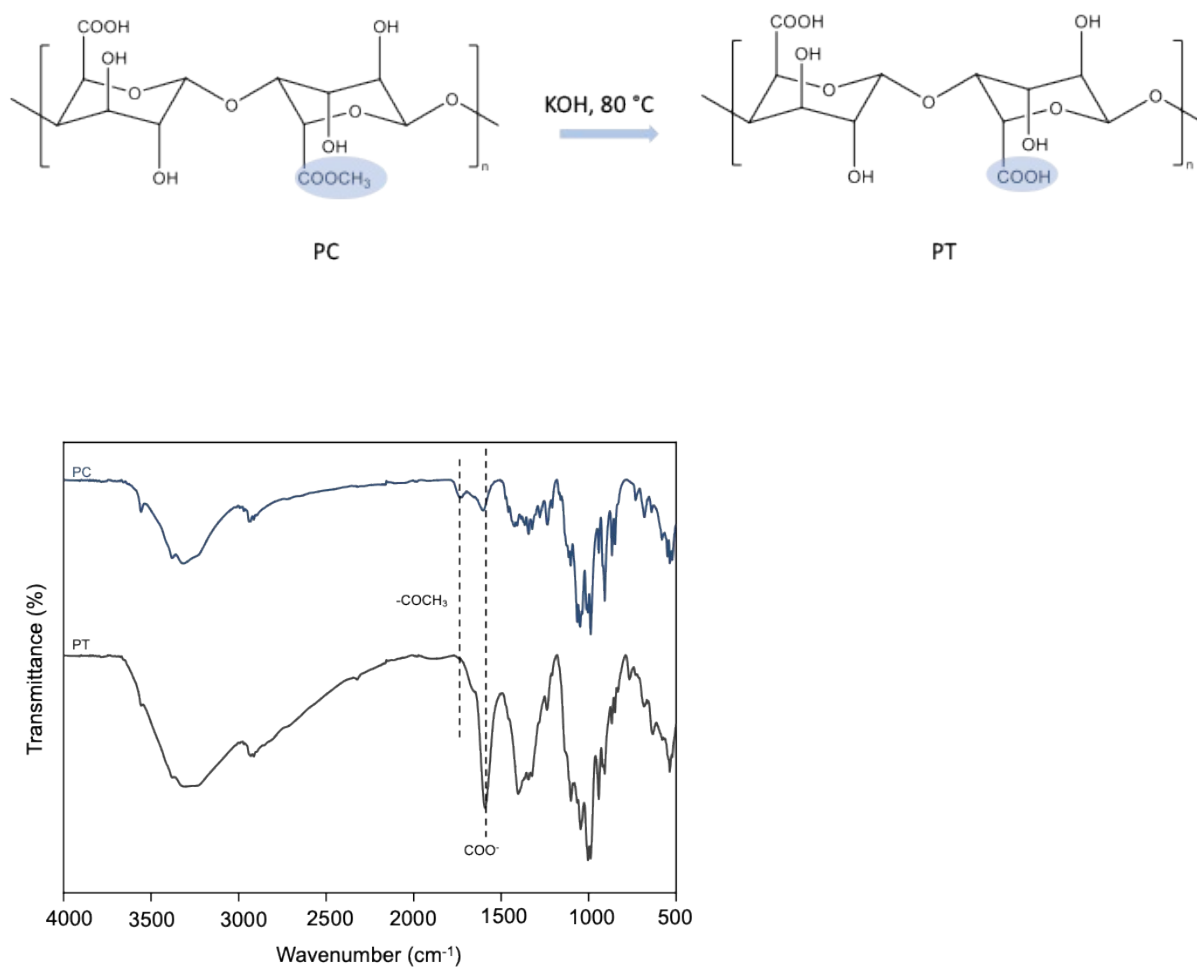


Figure S1. FTIR spectra for the conversion of PC to PT.

Supporting Information 2

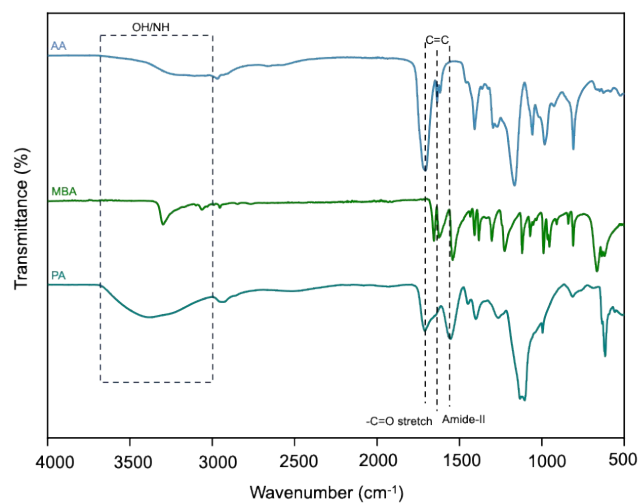


Figure S2. FTIR spectra for the conversion of AA to PA using MBA as the cross-linker, via free radical polymerisation.

Supporting Information 3

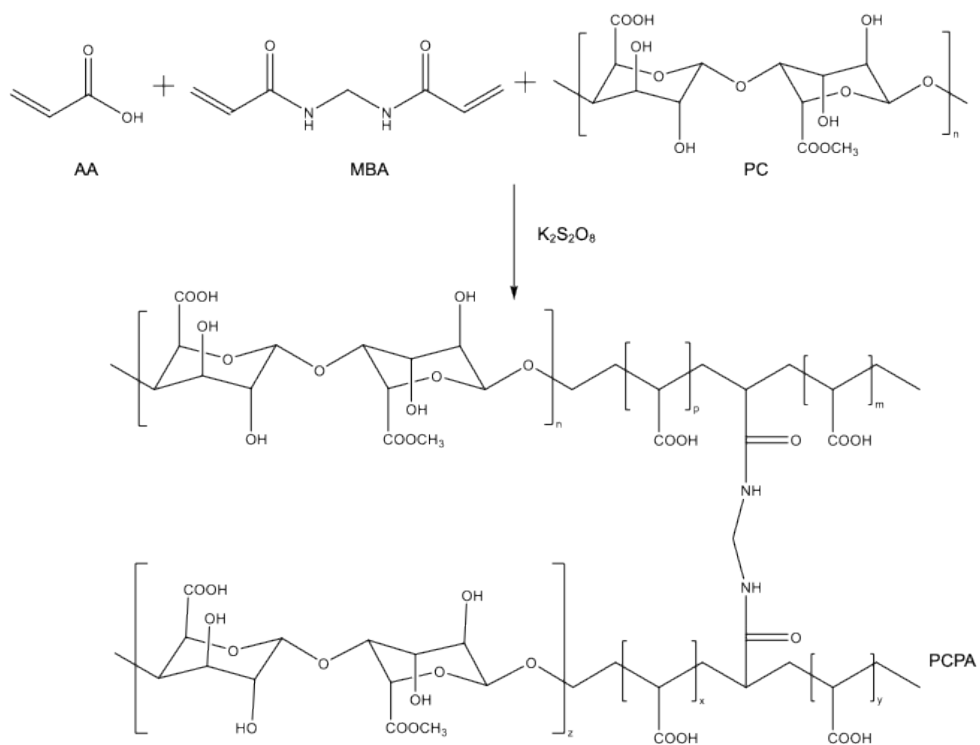
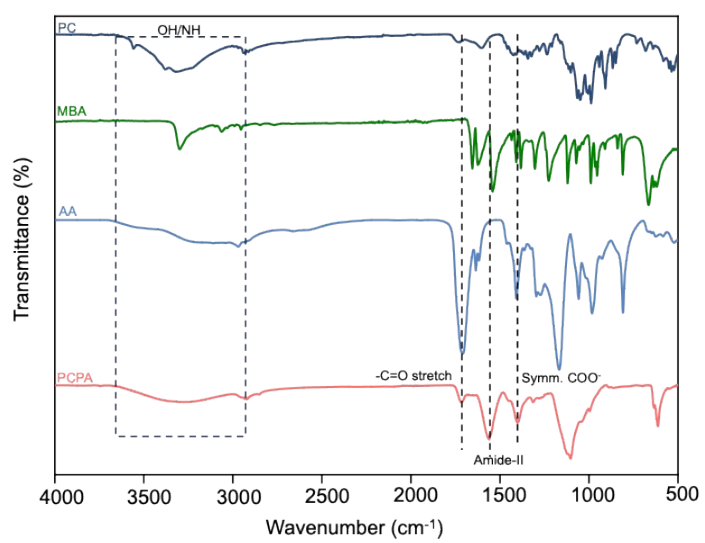


Figure S3. FTIR spectra for the functionalization of PC with AA using MBA as the cross-linker, via free radical polymerisation.



Supporting Information 4

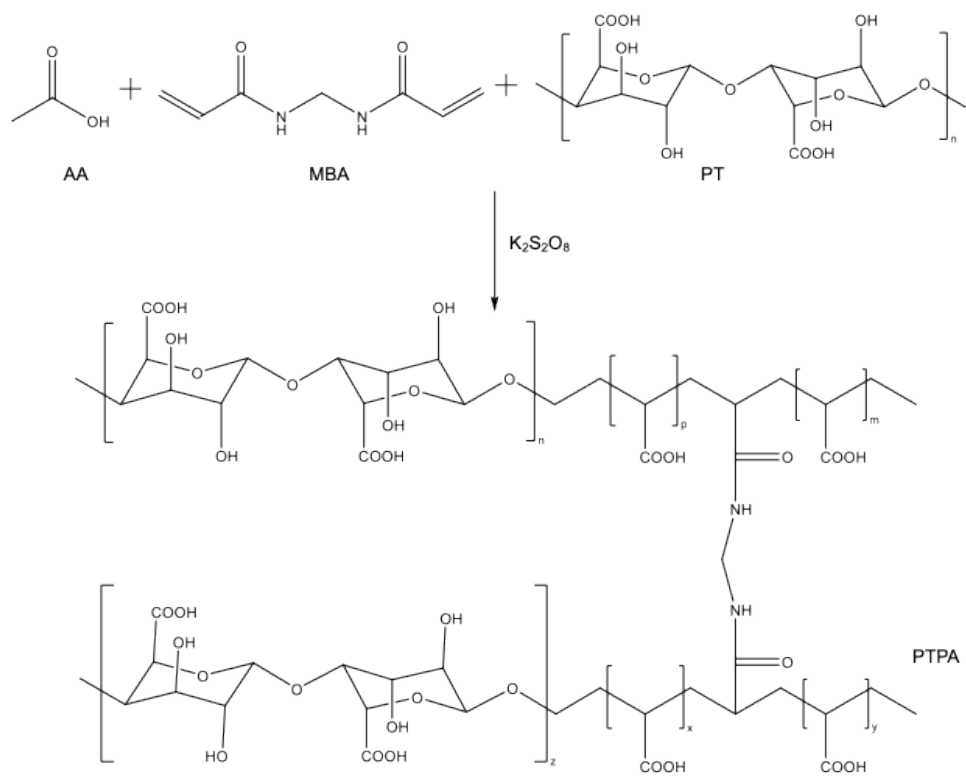


Figure S4. Grafting of PT to AA using MBA as the cross-linker.

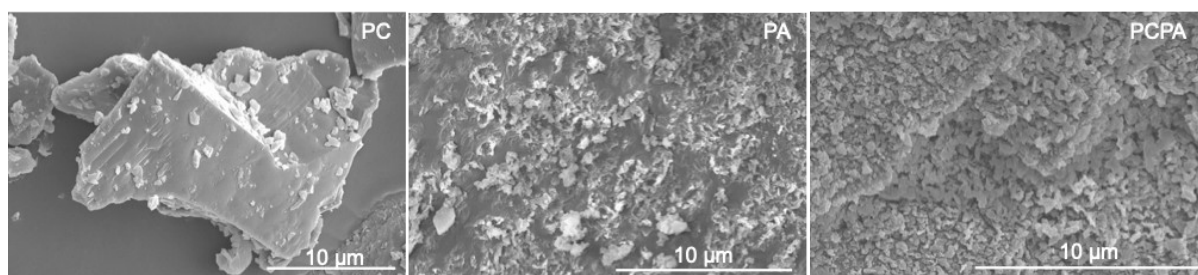


Figure S5. FESEM images of PC, PA and PCPA.

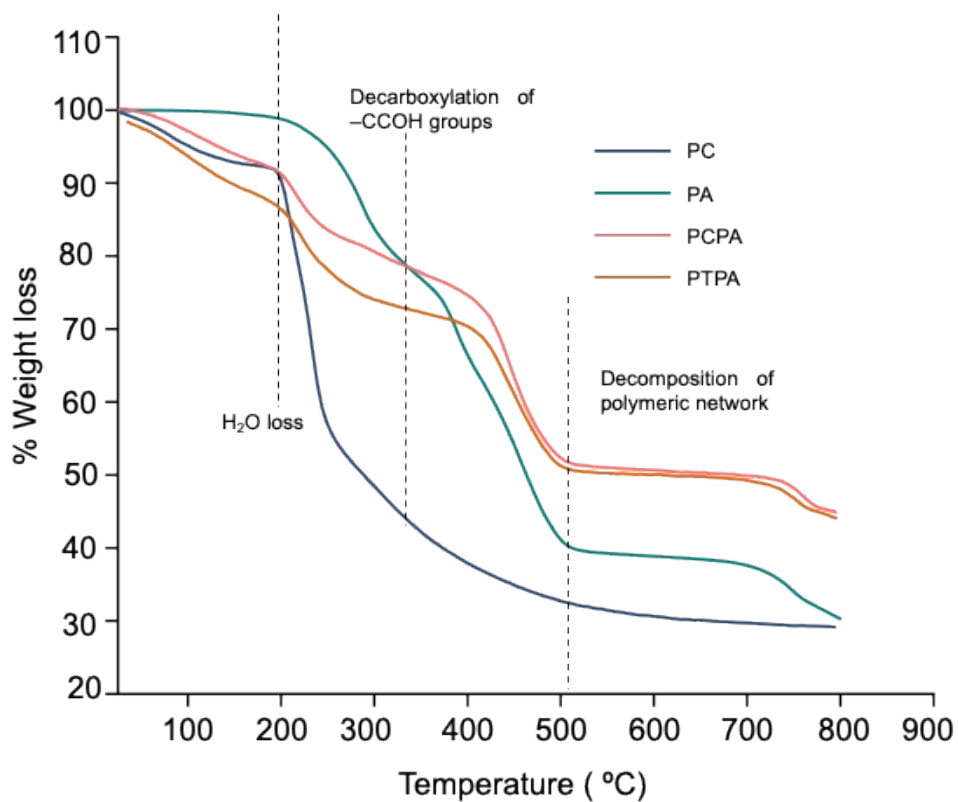


Figure S6. TGA thermograms of PC, PA, PCPA and PTPA under nitrogen atmosphere from room temperature to 800 °C.

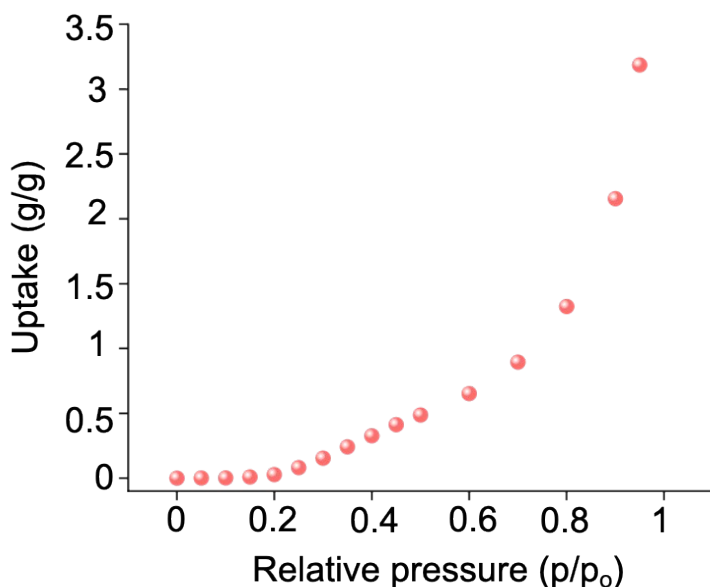


Figure S7. Sorption behaviour of PTPA at 293 K.

Moisture uptake of PTPA was measured over a range of relative humidity levels from 5% to 95% using a dynamic vapor sorption analyzer. As shown in Figure S7, PTPA exhibits a Type III sorption isotherm. Due to this Type III behaviour, it was not possible to reliably estimate the specific surface area from the adsorption data from the BET model.¹ We applied the Guggenheim-Anderson-de Boer (GAB) model^{2,3} for measuring the surface area of PTPA, which comes out to **190 m²/g**, using the equation

$$n = \frac{n_m C K a_w}{(1 - K a_w)(1 - K a_w + C K a_w)}$$

where n = adsorbed amount (g/g), a_w = relative humidity, n_m = monolayer adsorption capacity, C = heat constant of first layer, and K = multilayer constant.

The type III sorption behaviour indicates the presence of a polymeric network with accessible sites that interact strongly with water molecules. However, it was not possible to determine the pore size distribution from the water vapor sorption data. Further attempts were made to analyze PTPA using N₂ adsorption; however, no reliable data could be obtained. This was attributed to the hydrophilic nature of the material, where the polar functional groups did not interact effectively with non-polar N₂ molecules, leading to poor adsorption and

unreliable measurements. Also, significant water uptake was observed, confirming that adsorption was driven predominantly by specific chemical affinity between water molecules and the hydrophilic functional groups rather than physical pore confinement. Therefore, the combined evidences from the Type III isotherm profile, functional group chemistry, and selective interaction with water over N₂ suggested that water uptake in PTPA was primarily governed by chemical affinity rather than pore confinement

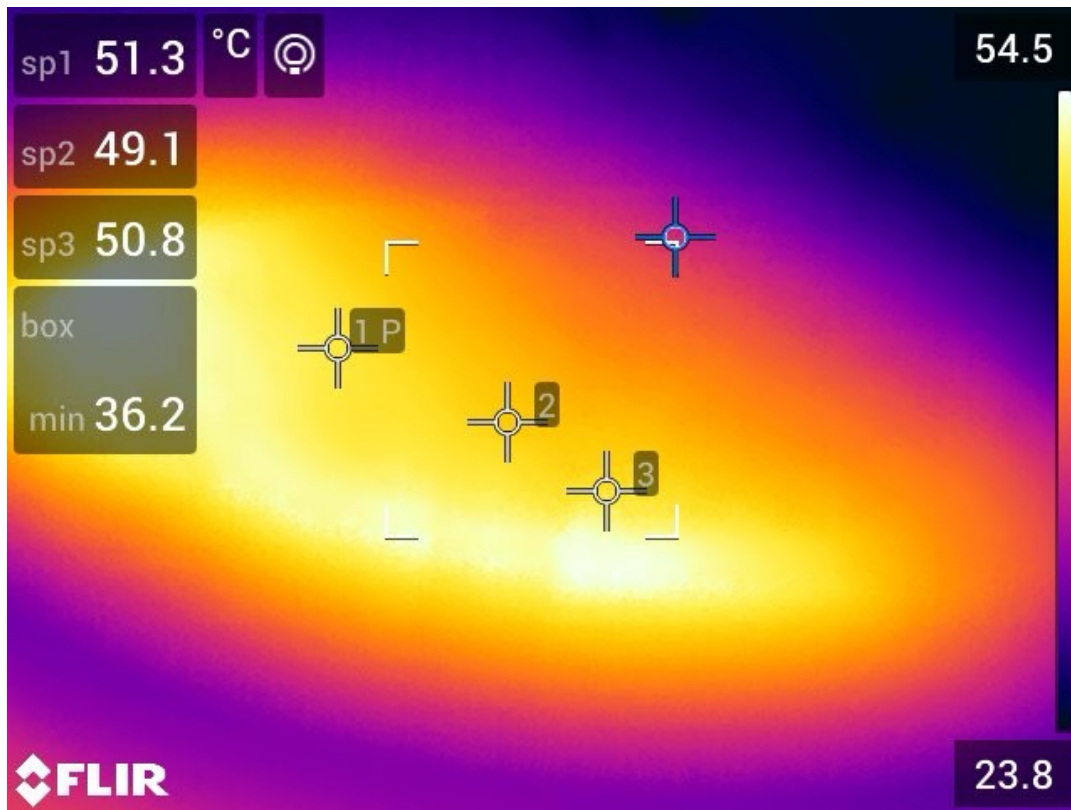


Figure S8. The surface temperature distribution of PTPA under 1 Sun. The colour gradient is indicated on the right. Temperatures at various points are marked.

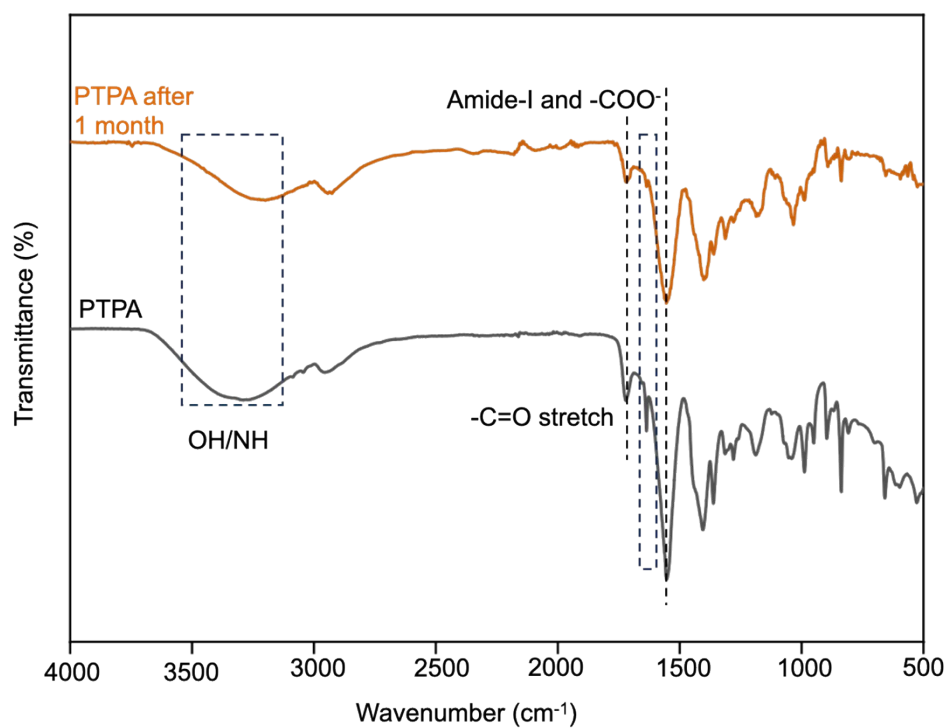


Figure S9. FTIR of PTPA freshly prepared and after keeping in normal environmental conditions for 1 month.

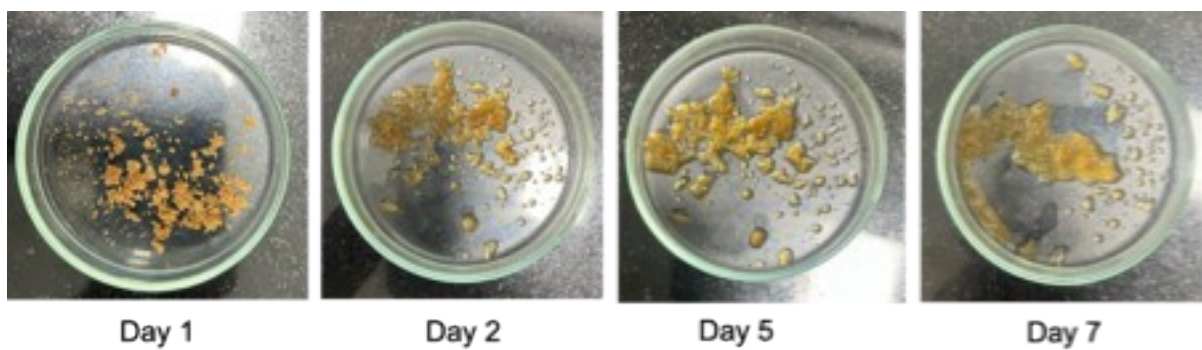


Figure S9. PTPA under 99% RH for 7 days.

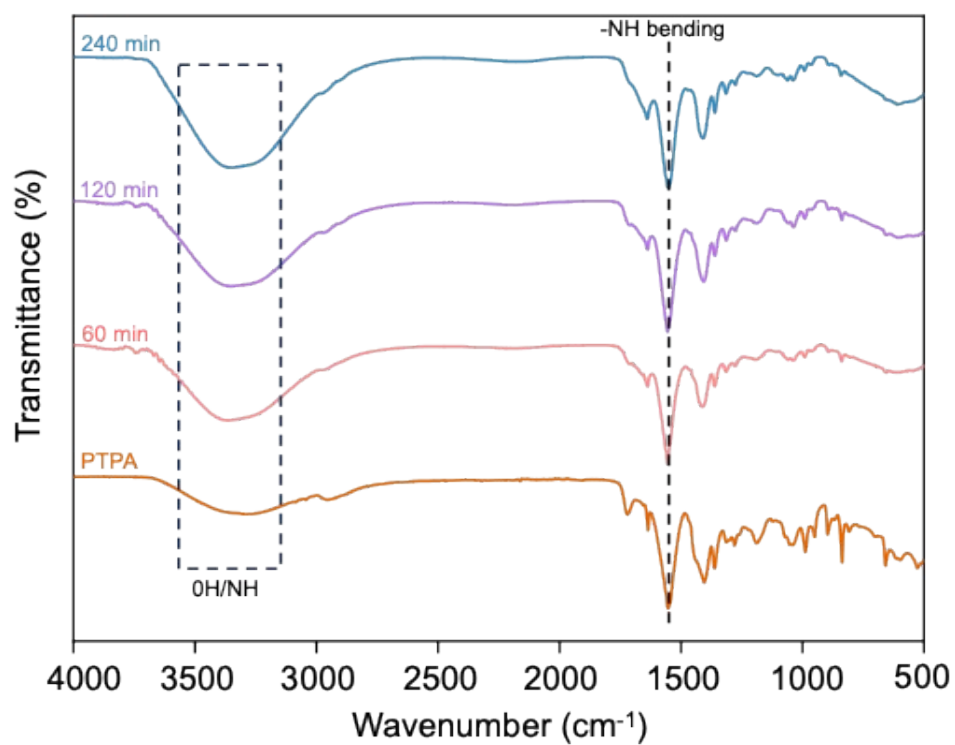
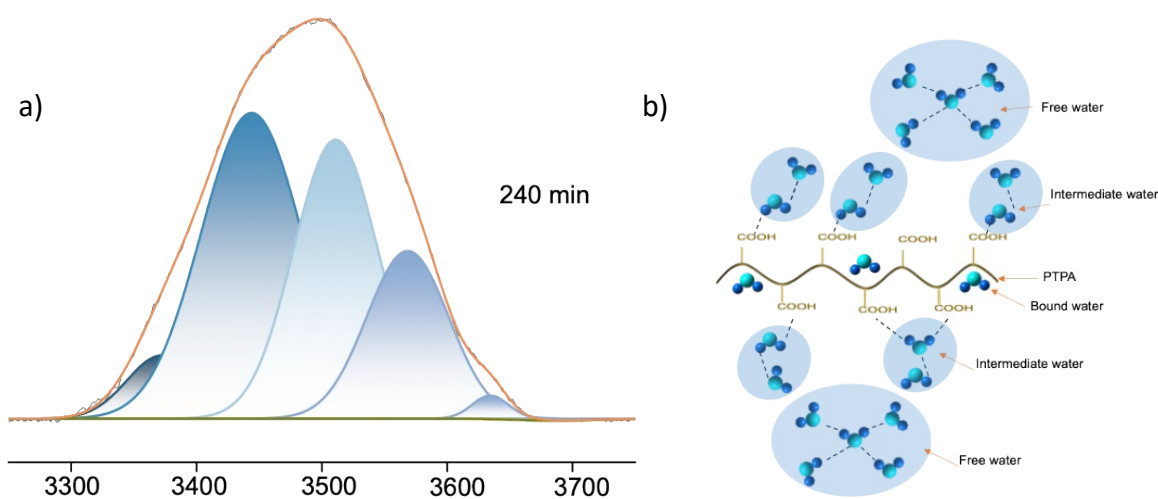


Figure S11. Time-dependent ATR-IR spectra of PTPA at regular time intervals on exposure to 99% RH.



Material Name	Raw materials	Cost (\$) per g of material	Cost (\$) of water (1 kg) in a	Reference

Figure S12. a) Deconvoluted Raman spectra of PTPA after 240 min of exposure to 99% RH, indicating the bound water, intermediate water and free water during hydration and swelling of the PTPA. b) Schematic illustration for the water sorption by PTPA.

Raman spectroscopy was done to elucidate the states of adsorbed water during hydration and swelling of the polymeric matrix. The nature of the water molecules varies depending on the interaction with the polymeric matrix. Bound water forms strong and stable hydrogen bond with the polymeric hydrogel, while the free water behaves similar to bulk water. In contrast, the intermediate water exhibits weaker hydrogen bond with the polymeric network, indicating the presence of bound and clustered water within the polymeric gel.

			day	
PTPA	Pectin, Acrylic acid, MBA, K ₂ S ₂ O ₈	0.027	13.5	Our work
CNF monolith	Cellulose, CaCl ₂	0.106	42.4	4
SNFs	TEOS, CTAB, PVP	0.233	100	5
LiCl-graphene-Cellulose	NFC, Graphene, LiCl	12.25	5100	6
CNT-PAM-CaCl ₂	AM, CaCl ₂ , Nanotube	0.037	21.38	7
Waste Corn stalk and LiCl	LiCl, Corn Stalk	0.038	-	8
ILCA	Loofah, CaCl ₂ , SA, Ink	0.026	17.8	9

Supporting Information 13

Table S1: Comparison of the adsorbent's costs and water production across different studies, based on lab-scale experiments.

Here, the cost of the water production per day is calculated based on the cost of the precursors used. No power consumption costs are being considered.

References

- 1 A. V. Smagin and N. B. Sadovnikova, *Polymers*, 2024, **16**, 593.
- 2 E. O. Timmermann, J. Chirife and H. A. Iglesias, *J. Food Eng.*, 2001, **48**, 19–31.

- 3 P. P. Lewicki, *Int. J. Food Sci. Technol.*, 1997, **32**, 553–557.
- 4 Y. Chen, Z. Yu, Y. Ye, Y. Zhang, G. Li and F. Jiang, *ACS Nano*, 2021, **15**, 1869–1879.
- 5 S. Kim, H. Park and H. Choi, *Microporous Mesoporous Mater.*, 2019, **281**, 23–31.
- 6 M. Wang, T. Sun, D. Wan, M. Dai, S. Ling, J. Wang, Y. Liu, Y. Fang, S. Xu, J. Yeo, H. Yu, S. Liu, Q. Wang, J. Li, Y. Yang, Z. Fan and W. Chen, *Nano Energy*, 2021, **80**, 105569.
- 7 R. Li, Y. Shi, M. Alsaedi, M. Wu, L. Shi and P. Wang, *Environ. Sci. Technol.*, 2018, **52**, 11367–11377.
- 8 F. Gong, H. Li, Q. Zhou, M. Wang, W. Wang, Y. Lv, R. Xiao and D. V. Papavassiliou, *Nano Energy*, 2020, **74**, 104922.
- 9 F. Deng, C. Wang, C. Xiang and R. Wang, *Nano Energy*, 2021, **90**, 106642.